Microsatellite instability in Arabidopsis increases with plant development

Golubov, A ; Yao, Y ; Maheshwari, P ; Bilichak, A ; Boyko, A ; Belzile, F ; Kovalchuk, I

Abstract: Plant development consists of the initial phase of intensive cell division followed by continuous genome endoreduplication, cell growth, and elongation. The maintenance of genome stability under these conditions is the main task performed by DNA repair and genome surveillance mechanisms. Our previous work showed that the rate of homologous recombination repair in older plants decreases. We hypothesized that this age-dependent decrease in the recombination rate is paralleled with other changes in DNA repair capacity. Here, we analyzed microsatellite stability using transgenic Arabidopsis (Arabidopsis thaliana) plants that carry the nonfunctional -glucuronidase gene disrupted by microsatellite repeats. We found that microsatellite instability increased dramatically with plant age. We analyzed the contribution of various mechanisms to microsatellite instability, including replication errors and mistakes of DNA repair mechanisms such as mismatch repair, excision repair, and strand break repair. Analysis of total DNA polymerase activity using partially purified protein extracts showed an age-dependent decrease in activity and an increase in fidelity. Analysis of the steady-state RNA level of DNA replicative polymerases , , Pol I-like A, and Pol I-like B and the expression of mutS homolog 2 (Msh2) and Msh6 showed an age-dependent decrease. An in vitro repair assay showed lower efficiency of nonhomologous end joining in older plants, paralleled by an increase in Ku70 gene expression. Thus, we assume that the more frequent involvement of nonhomologous end joining in strand break repair and the less efficient end-joining repair together with lower levels of mismatch repair activities may be the main contributors to the observed age-dependent increase in microsatellite instability.

DOI: https://doi.org/10.1104/pp.110.162933

Microsatellite Instability in Arabidopsis Increases with Plant Development[1][W][OA]

Andrey Golubov, Youli Yao, Priti Maheshwari, Andriy Bilichak, Alex Boyko, François Belzile, and Igor Kovalchuk*

Department of Biological Sciences, University of Lethbridge, Lethbridge, Alberta, Canada T1K 3M4 (A.G., Y.Y., P.M., A. Bilichak, A. Boyko, I.K.); and Department of Plant Science, Pavillon Charles-Eugène-Marchand, Université Laval, Laval, Quebec, Canada G1V 0A6 (F.B.)

Plant development consists of the initial phase of intensive cell division followed by continuous genome endoreduplication, cell growth, and elongation. The maintenance of genome stability under these conditions is the main task performed by DNA repair and genome surveillance mechanisms. Our previous work showed that the rate of homologous recombination repair in older plants decreases. We hypothesized that this age-dependent decrease in the recombination rate is paralleled with other changes in DNA repair capacity. Here, we analyzed microsatellite stability using transgenic Arabidopsis (*Arabidopsis thaliana*) plants that carry the nonfunctional β-glucuronidase gene disrupted by microsatellite repeats. We found that microsatellite instability increased dramatically with plant age. We analyzed the contribution of various mechanisms to microsatellite instability, including replication errors and mistakes of DNA repair mechanisms such as mismatch repair, excision repair, and strand break repair. Analysis of total DNA polymerase activity using partially purified protein extracts showed an age-dependent decrease in activity and an increase in fidelity. Analysis of the steady-state RNA level of DNA replicative polymerases α, δ, Pol I-like A, and Pol I-like B and the expression of mutS homolog 2 (*Msh2*) and *Msh6* showed an age-dependent decrease. An in vitro repair assay showed lower efficiency of nonhomologous end joining in older plants, paralleled by an increase in *Ku70* gene expression. Thus, we assume that the more frequent involvement of nonhomologous end joining in strand break repair and the less efficient end-joining repair together with lower levels of mismatch repair activities may be the main contributors to the observed age-dependent increase in microsatellite instability.

The genome of Arabidopsis (*Arabidopsis thaliana*) is extensively repetitive, which leads many to believe that Arabidopsis is subject to ancient autoploid events with many subsequent rearrangements and alterations (Meinke et al., 1998; Arabidopsis Genome Initiative, 2000; Blanc et al., 2000). Despite the highly reduplicated genome with the potential for a high degree of genetic redundancy, maintaining a consistent level of genome stability is critical. This is especially important when considering that plants do not have a predetermined germ line and that gametes are produced from meristematic cells that are products of many somatic cell divisions (Hays, 2002). Furthermore, as plants are sessile organisms, they are continuously exposed to various genotoxic elements such as heavy metals, reactive oxygen species, and UV irradiation. This constant exposure to harsh environmental conditions imposes a need for precise and efficient genome maintenance pathways, as the persistence of DNA damage and mutagenesis can decrease the fitness of current and future generations (Britt, 1996).

DNA mutagenesis cannot solely be attributed to environmentally induced genotoxic stress, as DNA is prone to spontaneous or replication-induced mutagenesis. For example, transitions of 5-methylcytosine to thymine are common spontaneous mutations (Britt, 1996), while DNA replication and repair infidelity can induce numerous errors (Sia et al., 1997; Tuteja et al., 2001). Hundreds of mutations are introduced upon each genome replication due to DNA polymerase infidelity. Repetitive elements are particularly prone to this type of mutation due to replication slippage, which refers to DNA polymerase dissociation during the replication of short repetitive sequences followed by the separation and subsequent reassociation of the daughter strand in a different but identical repeat (Viguera et al., 2001). Polymerase reloading and the resumption of DNA synthesis can result in addition or subtraction of the repeated sequence. Microsatellites, the simple tandem repeats of one to six nucleotides (Viguera et al., 2001), are highly susceptible to replication slippage.

The frequency at which these and other polymerase-derived errors persist depends largely on the DNA polymerase proofreading activity and the precision and fidelity of core DNA repair enzymes. Since many

[1] This work was supported by Natural Sciences and Engineering Research Council of Canada Discovery and Human Frontiers grants to I.K.

* Corresponding author; e-mail igor.kovalchuk@uleth.ca.

The author responsible for distribution of materials integral to the findings presented in this article in accordance with the policy described in the Instructions for Authors (www.plantphysiol.org) is: Igor Kovalchuk (igor.kovalchuk@uleth.ca).

[W] The online version of this article contains Web-only data.

[OA] Open Access articles can be viewed online without a subscription.

www.plantphysiol.org/cgi/doi/10.1104/pp.110.162933

repair pathways involve DNA polymerase activity, many of them can potentially contribute to an increase in microsatellite instability. Mismatch repair (MMR) is a repair mechanism involved in the correction of replication errors. It is essential for the maintenance of repeated sequences, as mutations in MMR genes are associated with a substantial destabilization of microsatellites (Karran, 1996), and in humans, microsatellite instability increases with aging (Ben Yehuda et al., 2000; Krichevsky et al., 2004; Neri et al., 2005).

The fidelity of different repair pathways can vary largely in the same or similar types of lesions. For example, single- and double-strand breaks can be repaired via homologous recombination (HR) or nonhomologous end joining (NHEJ) pathways (Britt, 1996; Tuteja et al., 2001; Kovalchuk et al., 2004; Boyko et al., 2006a). Of these pathways, HR is believed to be precise and largely error free, while NHEJ can induce numerous mutations ranging from single- to thousand-nucleotide insertions or deletions (Pelczar et al., 2003; Boyko et al., 2006b). It is unclear how either of these pathways is chosen for repair, but recent evidence from our laboratory suggests that the HR pathway is developmentally regulated, whereby NHEJ is up-regulated and HR is down-regulated with plant development (Boyko et al., 2006b). Currently, there is no information on whether other DNA repair pathways in plants are developmentally regulated.

Previous publications suggest that aging human cells have a higher frequency of mutations in microsatellites (Ben Yehuda et al., 2000; Krichevsky et al., 2004; Neri et al., 2005). No such data exist for plants. Here, we investigated microsatellite stability during the development of Arabidopsis using the *uidA* (GUS) reporter gene inactivated by an artificially incorporated microsatellite (Azaiez et al., 2006). We found a strong increase in instability with plant maturity. We tested the contributions of various repair pathways to age-dependent microsatellite instability and suggest that these changes are primarily due to more frequent involvement of the NHEJ pathway in DNA repair.

RESULTS

Older Plants Have Higher Rates of Microsatellite Instability

We analyzed microsatellite stability using the transgenic Arabidopsis reporter line 121A carrying the GUS gene interrupted by a 31-nucleotide insert comprising a stretch of 16 Gs (Azaiez et al., 2006). The insertion of this microsatellite results in a frameshift generating a premature stop codon (Fig. 1). Gene expression and the protein activity can be restored via deletion of one G nucleotide or insertion of two G nucleotides (Fig. 1).

To analyze whether the appearance of blue spots is the result of changes at the microsatellite locus, we have excised plant tissues with blue spots from lightly stained 3-week-old plants, prepared the DNA, amplified the region around the satellite using PCR techniques, cloned individual clones, and sequenced them. Out of 96 individual clones sent for sequencing, 64 gave readable sequences. Among those, 10 represented the wild-type sequence containing all 16 Gs, 22 had a single G deletion, two had a single G deletion and a single G→A mutation, 14 had a deletion of two Gs, eight had a deletion of three Gs, four had a deletion of four Gs, one had a deletion of five Gs, one had an insertion of one G, and two had an insertion of two Gs (Fig. 1C; Supplemental Fig. S1). To test whether these sequences are not sequence artifacts, we picked 10 random clones containing deletions/insertions of either one or several Gs and performed sequencing of the antiparallel strand; in all cases, we found similar results. Deletions seem to be a predominant type of revertant in this microsatellite region.

Next, we germinated plants from line 121A and harvested them for analysis of mutations at the reporter locus at 3, 5, 7, 10, 13, 16, 19, or 22 d post germination (dpg). We found that the number of blue spots increased dramatically with an increase in plant age; the number of events increased from 0.2 to 343 per plant (Fig. 2A; Supplemental Table S1). This increase could be simply attributed to the increase in the number of cells as well as the number of genomes carrying the target transgene.

To address this, we analyzed mutation rates (i.e. the number of events per single cell genome). To measure mutation rates in synthetic microsatellites, we first analyzed the number of genomes per cell in plants of different age. This analysis showed that the number of genomes increased from 1.13E+06 in 3-d-old plants to 3.02E+07 in 22-d-old plants (Supplemental Table S1). To obtain the mutation rate, we related the mutation frequency to the number of genomes and found that the mutation rate increased 64.2-fold from 1.77E−07 to 1.14E−05 in 3- and 22-d-old plants, respectively (Fig. 2B; Supplemental Table S1).

Since the mutation rate in microsatellite regions increases with age, it can be suggested that DNA repair in plants is indeed developmentally regulated. As mentioned above, mutations at microsatellite loci could be generated by many mechanisms, most of which can be related to mistakes attributable to replicative or repair DNA polymerases. To test this hypothesis, we measured DNA polymerase activity, DNA polymerase expression, repair efficiency, and the expression of various DNA repair genes.

Higher Microsatellite Mutation Rates Are Not Due to Lower DNA Polymerase Activity in Older Plants

To analyze whether older plants have lower levels of DNA polymerase activity, we used a DNA polymerase activity assay. This assay is based on the ability of a freshly prepared protein extract to extend the DNA sequence of a 15-nucleotide primer upon annealing to a complementary 30-nucleotide template (Supplemental Fig. S2). Incubation of the extract with the template,

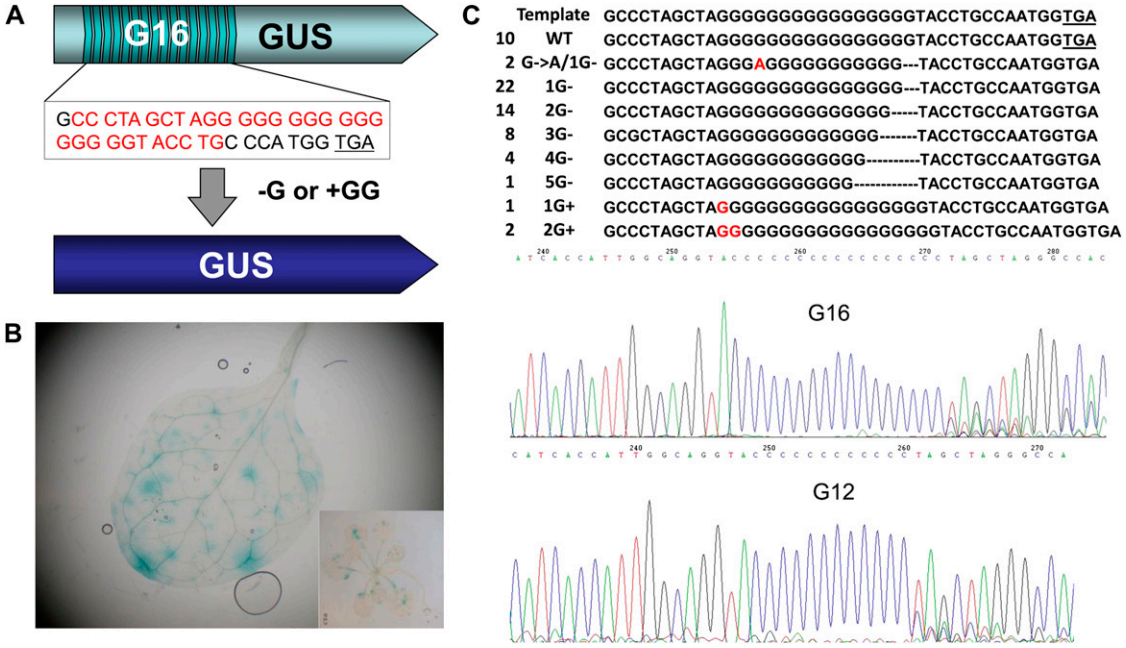

Figure 1. Schematic presentation of the construct for the analysis of microsatellite instability. A, Insertion of the sequence (in red) carrying the G16 microsatellite results in the frameshift leading to an in-frame stop codon a couple of nucleotides downstream. Deletion of one G or insertion of two Gs would restore the open reading frame of the GUS gene and thus activate the protein. B, Cells and their progeny in which reading-frame restoration occurred can be visualized after histochemical staining as blue sectors. The image shows the leaf of a 21-d-old plant with a number of blue sectors. The inset shows the entire plant. C, Analysis of the types of reversions occurring at the microsatellite region of the GUS transgene. The numbers show the frequency of occurrence of a particular sequence. A template represents the sequence of the plasmid used to produce line 121A. WT identifies a wild-type sequence, whereas G→A/1G−, 1G−, 2G−, 3G−, 4G−, 5G−, 1G+, and 2G+ represent mutations. The bottom of the figure shows representative chromatograms for the wild-type sequence (G16) and deletion of four Gs (G12).

the primer, and a mix of dGTP and dATP results in extension of the primer by two nucleotides. Thus, the appearance of a 17-nucleotide extension product is expected, whereas the appearance of products larger than 17 nucleotides (e.g. 18 nucleotides) would indicate misincorporation of nucleotides. The assay allows the analysis of both DNA polymerase activity, the ability to incorporate nucleotides into a growing DNA chain, and DNA polymerase fidelity, the ability to incorporate correct nucleotides. To decrease the number of samples, we used protein extracts from tissue harvested at 5, 12, and 22 dpg. Figure 3A shows a representative image of the assay. The 15-nucleotide product corresponds to the FAM-labeled primer, the 17-nucleotide product represents the extended primer that incorporated precisely two nucleotides, G and A, whereas the 18-nucleotide product results from the incorporation of three nucleotides, G, A, and another misincorporated nucleotide, either A or G (Fig. 3A).

Analysis of the intensity of the 17-nucleotide product showed that DNA polymerase activity inversely correlated with plant age; the older the plants, the lower the DNA activity (Fig. 3, A, B, and E). Analysis of the intensity of the 18-nucleotide product also showed a substantial age-dependent decrease in product intensity (Fig. 3, A and C). Relative DNA polymerase fidelity was calculated by relating the intensity of the 18-nucleotide product (due to misincorporation) to the intensity of the 17-nucleotide product (precise extension) and then standardizing it to the 5-dpg sample. The analysis showed that 12-d-old plants had comparable DNA polymerase fidelity, whereas 21-d-old plants had a 75% increase in fidelity (Fig. 3F).

While analyzing gel images, we noticed the presence of shorter molecules of less than 15 nucleotides. We hypothesized that the appearance of these fragments was due to exonuclease and endonuclease activities (Fig. 3A). The analysis of the intensity of fragments of the three-nucleotide product showed that the extracts prepared from 5-d-old plants had much higher nuclease activity than those prepared from 12- or 21-d-old plants (Fig. 3, A and D). Thus, we concluded that younger plants had higher exonucleolytic/endonucleolytic activities (Fig. 3G).

Steady-State RNA Levels of Genes Coding DNA Polymerases Are Age Dependent

The aforementioned assay gave us a global picture of DNA polymerase activity and fidelity. Unfortunately, it was difficult to decipher the contribution of an individual DNA polymerase in the assay described

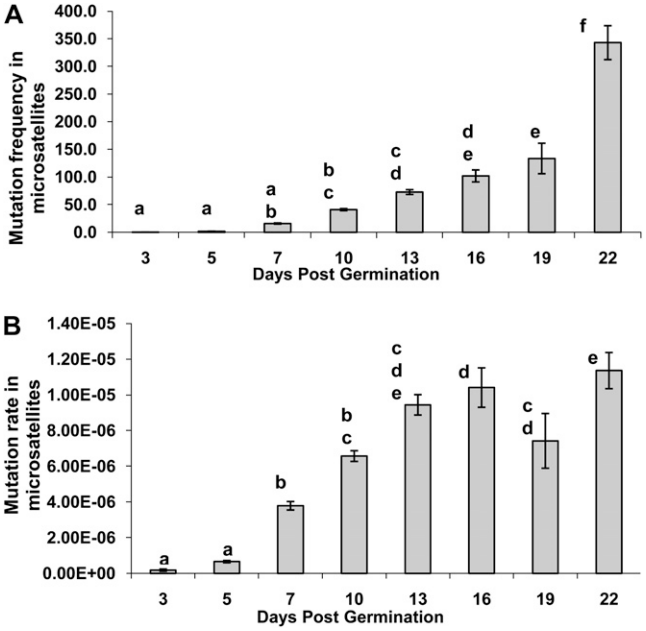

Figure 2. Mutation frequency and mutation rates at microsatellite loci increase with age. Seeds of transgenic Arabidopsis plants were germinated and grown on Murashige and Skoog medium. Plants were harvested for histochemical staining at 3, 5, 7, 10, 13, 16, 19, and 22 dpg. A, The graph shows the average mutation frequency (as calculated from three independent experiments), and error bars indicate SE. Mutation frequency was calculated as the average number of mutation events (blue spots) per the number of plants used for the analysis. The values that are not connected by the same letter are significantly different (Student's *t* test, $\alpha = 0.05$). B, The graph shows the average mutation rate (as calculated from three independent experiments), and error bars indicate SE. The mutation rate was calculated by relating mutation frequency to the total number of genomes present in plants of different ages. The values that are not connected by the same letter are significantly different (Student's *t* test, $\alpha = 0.05$).

above. We hypothesized that changes in activity in older plants were in part due to changes in the expression of various DNA polymerases. A decrease in DNA polymerase expression in older plants would lead to less protein available for DNA synthesis. Since in our assay it was impossible to find out which DNA polymerases were involved in DNA synthesis, we checked the steady-state RNA level of the following DNA polymerases: α, δ, θ, η, κ, λ, Pol AtREV1, Pol I-like A, and Pol I-like B. The analysis showed an age-dependent decrease in the expression of replicative DNA polymerases α, δ, Pol I-like A, and Pol I-like B (Table I). The expression of bypass DNA polymerases η, κ, and AtREV1 varied, whereas the expression of Pol η decreased, the expression of Pol κ did not change, and the expression of AtREV1 actually increased with age. The expression of the translesion DNA polymerase AtREV3 increased in 12- and 21-d-old plants, whereas the expression of the translesion Pol θ increased only in 21-d-old plants. Finally, the expression of the DNA repair and recombination DNA Pol λ also increased with age. Replicative DNA polymerases are the most abundant and active in developing organisms. Thus, it is not surprising to find a correlation between a decrease in the expression of replicative DNA polymerases and a decrease in global DNA polymerase activity. As we mentioned above, microsatellite instability can be the result of mistakes in replication or DNA repair. Such repair mechanisms could include mismatch repair, nucleotide excision repair, and strand break repair. Next, we decided to test the contribution of these repair processes to higher mutation rates at microsatellite loci.

Mistakes in Mismatch Repair Are Unlikely To Be the Reason for Higher Microsatellite Instability in Older Plants

To analyze the possible involvement of MMR, we performed two experiments. First, we crossed the 121A line to an *msh2* (for mutS homolog 2) mutant, selected homozygous plants, and analyzed microsatellite instability in plants of various ages. We hypothesized that if MMR is responsible for the higher rate of mutations at microsatellite loci, complete loss of MMR activity seen in the mutant should result in a much greater increase in the mutation rate in young leaves relative to older leaves. The analysis showed that *msh2* in general had higher microsatellite instability as compared with wild-type plants. However, the difference between old *msh2* plants and young plants was similar to that in wild-type plants; there was approximately a 70-fold increase in the mutation rate in *msh2* plants at 22 dpg versus 3 dpg, as compared with a 64-fold increase in wild-type plants (Supplemental Table S2). It has to be noted, however, that since the average number of events in plants increased substantially, it became too difficult to count individual events in each plant (the average number of events in 22-d-old plants was well over 500). We thus cannot completely exclude that older *msh2* plants may have a greater mutation rate increase at the microsatellite locus of the GUS transgene as compared with wild-type plants.

Next, we tested the expression of genes coding for mismatch repair proteins, MSH2, MSH6, and MSH7. The analysis of steady-state RNA levels showed an age-dependent decrease in the *MSH2* and *MSH7* genes and a tendency to an increase in the *MSH6* gene (Table II).

Older Plants Have Less Active Excision Repair

To test the possible contribution of base excision repair (BER) toward an increase in microsatellite instability, we performed the BER and nucleotide excision repair (NER) assays using extracts prepared from 5-, 12-, and 21-d-old plants. The assay is based on the ability of partially purified protein extracts to perform the repair of nondamaged or UV-damaged circular or linear plasmid DNA. Incubation of the plasmid DNA with protein extracts from 5-, 12-, and 21-d-old plants

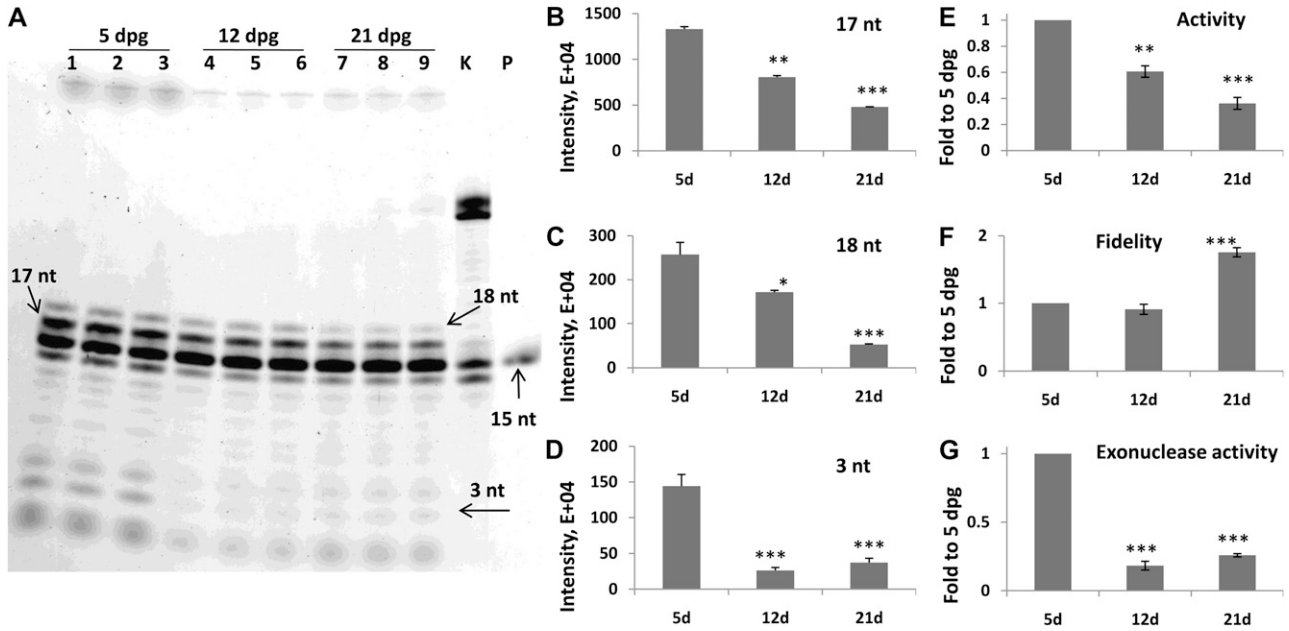

Figure 3. Analysis of DNA polymerase activity and fidelity in plants of different ages. A, Extracts from 5-, 12-, and 21-d-old Arabidopsis plants (ecotype Columbia) were incubated in triplicate with 2 mM dGTP + dATP. The three-, 15-, 17-, and 18-nucleotide (nt) bands are indicated by arrows. K, Klenow fragment reaction products; P, the 15-nucleotide 6-FAM-labeled primer only. B, The average intensity (in arbitrary units ± SD) of the 17-nucleotide band. Asterisks show significant differences in 12- and 21-d-old plants as compared with 5-d-old plants (** $P < 0.01$, *** $P < 0.001$). C, The average intensity (in arbitrary units ± SD) of the18-nucleotide band. Asterisks show significant differences in 12- and 21-d-old plants as compared with 5-d-old plants (* $P < 0.05$, *** $P < 0.001$). D, The average intensity (in arbitrary units ± SD) of the three-nucleotide band. Asterisks show significant differences in 12- and 21-d-old plants as compared with 5-d-old plants (*** $P < 0.001$). E, DNA polymerase activity (fold) is calculated by relating the intensity of the 17-nucleotide band in 12- and 21-d-old plants to the intensity of this band in 5-d-old plants. Bars show the average of three experiments with SD. Asterisks show significant differences in 12- and 21-d-old plants as compared with 5-d-old plants (** $P < 0.01$, *** $P < 0.001$). F, DNA polymerase fidelity (fold) is calculated by relating the intensity of the 18-nucleotide band (as shown in C) to the intensity of the 17-nucleotide band (as shown in B). The data for 12- and 21-d-old plants are shown as fold change compared with 5-d-old plants. Bars show the average of three experiments with SD. Asterisks show significant differences in 21-d-old plants as compared with 5-d-old plants (*** $P < 0.001$). G, Exonuclease activity (fold) is calculated by relating the intensity of the three-nucleotide band in 12- and 21-d-old plants to the intensity of this band in 5-d-old plants. Bars show the average of three experiments with SD. Asterisks show significant differences in 12- and 21-d-old plants as compared with 5-d-old plants (*** $P < 0.001$).

showed that repair efficiency of circular DNA was dramatically lower in 21-d-old plants as compared with 5- or 12-d-old plants (Fig. 4). The rate of incorporation of radionuclides into blunt-cut or nonsticky-end-cut linear DNA was higher than in circular DNA. These types of strand breaks are typically repaired via end-joining repair. In both cases, however, 21-d-old plants showed lower incorporation rates as compared with younger plants (Fig. 4). Repair of a UV-damaged substrate showed yet higher band intensities, which presumably reflects BER/NER repair of UV-damaged DNA. In this case, however, band intensity was the highest in 5-d-old plants; it was the lowest in 21-d-old plants, while in 12-d-old plants, it was intermediate. A decrease in band intensity would suggest less frequent involvement of BER/NER and possibly would reflect the higher number of DNA damages that remain unrepaired. As one of the steps of BER/NER involves the DNA polymerase function and as DNA polymerase activity decreases with age, it is possible that the age-dependent decrease in BER/NER efficiency is at least in part due to lower DNA polymerase activity. A higher frequency of mutations at microsatellite loci in older plants could be due to more frequent involvement of BER/NER and thus more frequent mistakes of BER/NER. Since what we observed was the exact opposite, we have concluded that higher microsatellite instability in older plants is not due to increased involvement of BER/NER.

Higher Rates of Mutations at Microsatellite Loci Could Be Due to More Frequent Involvement of NHEJ Repair in Arabidopsis

To test whether the involvement of NHEJ has any effect on the frequency of microsatellite stability, we tested the ability of protoplasts prepared from young and old plants to repair double-strand breaks. We used

Table I. *The steady-state RNA levels of genes coding for various DNA polymerases*

The real-time PCR data for each DNA polymerase were related to the *RCE1* data and then standardized to the data from 5-d-old plants (taken as 1.0). The data represent averages of three independent experiments with SD. The asterisks show significant differences as compared with the data from 5-d-old plants: * $P < 0.05$, ** $P < 0.01$, *** $P < 0.001$.

Gene	5 d	12 d	21 d
Pol α	1 ± 0.064	0.24 ± 0.006***	0.21 ± 0.010***
Pol δ	1 ± 0.062	0.64 ± 0.034**	0.69 ± 0.070*
Pol I-like A	1 ± 0.073	1.04 ± 0.062	0.56 ± 0.182*
Pol I-like B	1 ± 0.080	0.66 ± 0.038**	0.69 ± 0.029**
AtREV1	1 ± 0.033	2.34 ± 0.066***	2.47 ± 0.058***
AtREV3	1 ± 0.052	0.77 ± 0.161	1.20 ± 0.062*
Pol κ	1 ± 0.081	0.69 ± 0.089*	0.66 ± 0.074*
Pol η	1 ± 0.111	0.95 ± 0.097	0.94 ± 0.045
Pol θ	1 ± 0.078	2.84 ± 0.182***	2.02 ± 0.080***
Pol λ	1 ± 0.102	0.44 ± 0.290*	0.18 ± 0.034***

this assay in the past to show the differential efficiency of strand break repair in plant and animal cells (Pelczar et al., 2003; Kovalchuk et al., 2004). For the analysis, protoplasts of 5-, 12-, and 21-d-old plants were transfected with 5 μg of linear DNA serving as a template for strand break repair. Our previous experiments showed that the peak of extrachromosomal strand break repair occurs between 4 and 12 h post transfection (Pelczar et al., 2003). Therefore, we incubated DNA with protoplasts for 4 and 12 h. Next, the DNA prepared from protoplasts was used for *Escherichia coli* transfection.

Any difference between the numbers of ampicillin-resistant bacteria obtained from transfection with the DNA recovered from plants of different ages would be a reflection of the efficiency of strand break repair. The analysis showed more ampicillin-resistant bacteria obtained from transfection of older protoplasts; a nearly 50% increase between 5 and 21 dpg was observed (Fig. 5A). Next, we analyzed the percentage of white colonies among all white and blue colonies. The appearance of blue colonies is expected if break repair is faithful, whereas the appearance of white colonies would indicate deletions and insertions of various sizes reflecting error-prone repair. The analysis showed that in 21-d-old plants, the percentage of white colonies was over 1.5-fold higher as compared with 5-d-old plants (Fig. 5B). This experiment suggested that older plants had the increased strand break repair activity but lower fidelity.

Next, we analyzed the steady-state levels of *Ku70* and *Rad51* RNAs and found that the expression of *Ku70* increased and the expression of the *Rad51* gene slightly decreased with plant age (Fig. 6A). Analysis of protein levels also showed that the amount of KU70 protein increased with age (Fig. 6, B and C). We attempted to perform western-blot analysis for RAD51; unfortunately, two sets of generated antibodies were too unspecific to draw any conclusion.

These experiments suggest that the contribution of NHEJ to strand break repair becomes more frequent and evident with age. Previously, we indirectly showed that HR repair decreased with age (Boyko et al., 2006b). Since these two repair pathways compete for the same substrate (strand breaks), it makes sense that NHEJ repair has to compensate for the decreased involvement of HR.

DISCUSSION

Here, we report that older plants have an increased frequency of microsatellite instability as compared with younger plants and propose that this increase is associated with a more frequent contribution of the error-prone NHEJ pathway toward strand break repair.

Deletions Are the Predominant Type of Mutations at the Artificial Microsatellite Loci

Our analysis showed that the majority of mutations observed at the microsatellite locus of the GUS transgene were deletions; among 54 mutated sequences, there were only three insertions and 51 deletions. Thus, deletions occurred up to 16 times more frequently than insertions. When starting the experiments, we assumed that GUS protein activity would

Table II. *The steady-state RNA levels of genes coding for mismatch repair proteins*

The real-time PCR data for each gene were related to the *RCE1* data and then standardized to the data from 5-d-old plants (taken as 1.0). The data represent averages of three independent experiments with SD. The asterisks show significant differences as compared with the data from 5-d-old plants: * $P < 0.05$, ** $P < 0.01$, *** $P < 0.001$.

Gene	5 d	12 d	21 d
MSH2	1 ± 0.082	0.43 ± 0.023***	0.41 ± 0.017***
MSH6	1 ± 0.069	1.10 ± 0.015	1.16 ± 0.057*
MSH7	1 ± 0.147	0.23 ± 0.092**	0.33 ± 0.023***

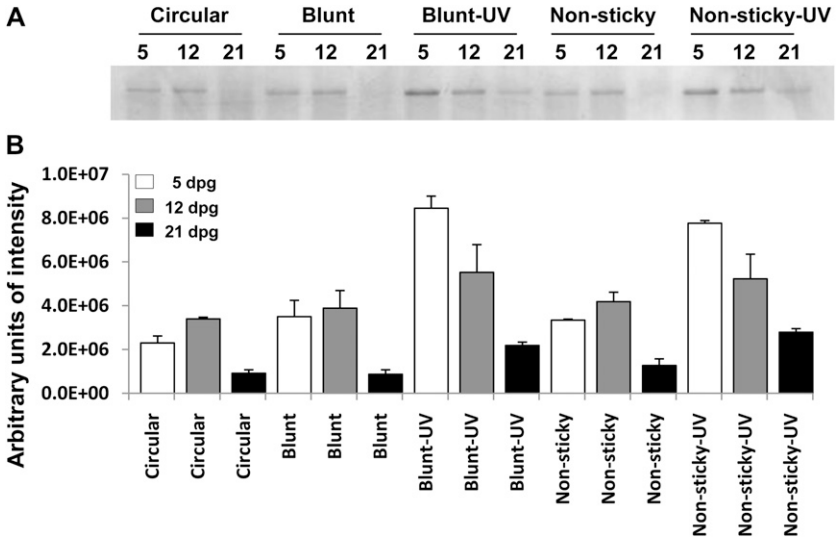

Figure 4. The in vitro DNA repair assay shows the lower excision repair capacity of older plants. The DNA repair assay was performed by incubation of circular and linear nonexposed and UV-irradiated DNA with partially purified protein extracts prepared from 5-, 12-, and 21-d-old plants. A, A representative gel. Circular shows the band stemming from the incorporation of digoxigenin-labeled dNTPs into circular DNA incubated with protein extracts. Blunt, Blunt-UV, Non-sticky, and Non-sticky-UV show the bands stemming from the incorporation of dNTPs into blunt-cut DNA, blunt-cut UV-irradiated DNA, nonsticky-end-cut DNA, and nonsticky DNA irradiated with UV light. B, Units of the average band intensity as seen in A prorated to the loading controls (Supplemental Fig. S3). The data are shown as averages (calculated from three independent experiments with SD).

be predominantly restored via a deletion of a single G or an insertion of two Gs. Whereas the former was a frequent case (24 out of 54 mutated sequences had a single G deleted), the latter was a rare event, with only two cases having an insertion of two Gs. We were surprised to find clones representing deletions of two and three Gs (these events represented 22 out of 54 sequences with mutations). It is hardly possible that these sequences would lead to the restoration of the GUS+ phenotype, as they would not restore the coding frame. Since it was difficult to excise blue sectors only, it is possible that some "nonblue" tissues have been PCR amplified. Since reversions at one allele of 121A reporter plants would be sufficient to activate the transgene, the second copy could also mutate, not necessarily in the same manner; thus, it is possible that the events representing deletions of two or three Gs could have occurred at the second allele.

Curiously, data exist that show that deletions are indeed more common in the microsatellite regions. An in vitro analysis of replication showed that the frequency of mutations at (A)n and (CA)n microsatellites directly correlated with the number of repeats, and it was higher for single rather than dual nucleotide repeats. The frequency of the mutations observed was as high as one in 100 replicated repeats, with the contraction rate for (A)n and (CA)n being 5- and 12-fold higher than the expansion rate, respectively (Shinde et al., 2003). Similarly, the analysis of mutation types at microsatellites in wheat (*Triticum aestivum*) showed that deletions at the microsatellite loci were 4-fold more frequent than insertions (Thuillet et al., 2002).

Age-Dependent Changes in DNA Repair Efficiency in Different Organisms

In our experiments, we observed that the rate of mutations at artificial microsatellite loci of a transgene increases with plant age. It is difficult to draw any parallel with the findings reported in the literature because similar studies have not been performed. The effect of aging on DNA repair and mutation rates was primarily studied in seeds. Embryo cells within plant seeds do not divide and exist in the G_0/G_1 stage of the cell cycle for a long period of time (Whittle et al., 2001). Since it is possible to manipulate the duration of the resting stage in seeds, the assessment of the physiological and genetic impact of cell aging on DNA damage and mutation rates is also possible. Several papers studying the impact of seed age on the onset of mutations support our finding (for review, see Whittle and Johnston, 2006). Naturally aged rye (*Secale cereale*) seeds have increased variations in amplified fragment length polymorphisms and other genetic markers (Chwedorzewska et al., 2002a, 2002b). Plantlets of *Zea mays* (Peto, 1933), *Triticum* (Melletti and Russo, 1969), and *Crepis* (Boldyrev et al., 2004) germinated from older seeds contain higher levels of chromosome rearrangements and other mutations.

However, age-dependent changes in the efficiency of DNA repair in plants have not yet been reported. Analysis of mutation rates in germinated plants is more difficult, since cell divisions are not synchronized and plant cells have various degrees of endoreduplication. But older plants contain higher percentages of older cells. The mutation rate is also more difficult to study in living plants due to the rare occurrence of single nucleotide changes. It was estimated that mutations at a given nucleotide of the transgene occur at the rate of 10^{-8} to 10^{-9}. Given the fact that a 3-week-old Arabidopsis plant of an average size contains about 10^6 cells, it becomes clear that measuring mutation rates is a difficult process. However, cell genomes contain stretches of simple sequence repeats, microsatellites that mutate at a much higher rate (Marriage et al., 2009). It was estimated that mutation rates at microsatellites were 10^3- to 10^4-fold higher than mutation rates at nonrepetitive sequences.

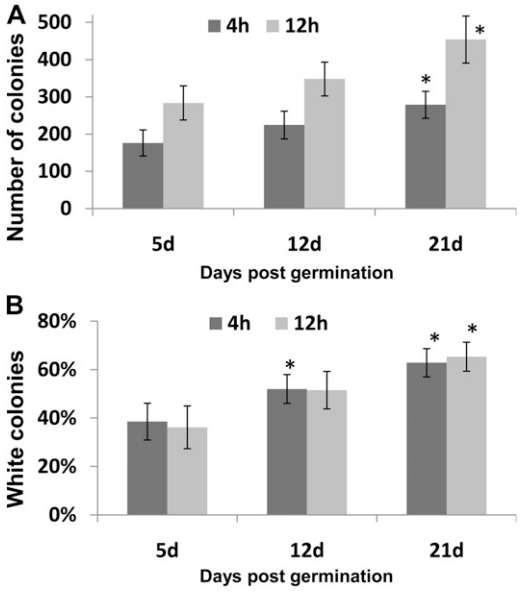

Figure 5. The fidelity of strand break repair is lower in protoplasts prepared from older plants. Protoplasts prepared from leaves of 5-, 12-, and 21-d-old plants were transfected with linear plasmid DNA. At 4 and 12 h post transfection, bacterial cells were transformed with repaired circular DNA, and the number of white and blue colonies was calculated. A, Average number of colonies (blue and white) as counted from three independent experiments (with SD). The asterisks show significant differences ($P < 0.05$) in 12- and 21-d-old plants as compared with 5-d-old plants. B, The average (with SD) percentage of white colonies of all colonies was calculated from three independent experiments. The asterisks show significant differences ($P < 0.05$) in 12- and 21-d-old plants as compared with 5-d-old plants.

Thus, the analysis of mutation rates can be easily done via the analysis of mutations at the microsatellite loci. Indeed, we utilized a method for the detection of mutations at the artificial microsatellite loci cloned into the GUS transgene and found that older plants had higher rates of mutations in these regions.

The data on the mutation rate in animals are much more complete and suggest that aging animal cells have a lower efficiency of most types of DNA repair, including excision repair, mismatch repair, and strand break repair mechanisms (Gorbunova et al., 2007). Mitchell and Hartman (1990) showed that proliferating tissues had a higher repair capacity as compared with terminally differentiated nondividing cells (Mitchell and Hartman, 1990). More specifically, it was found that senescent cells in G_0/G_1 do not use HR for strand break repair; thus, they more often rely on the use of the NHEJ pathway (Seluanov et al., 2007). Analysis of excision repair capacity also showed age dependence. An in vitro assay measuring repair efficiency of a synthetic DNA substrate containing a single G:U mismatch detected a strong decline in BER activity in brain, liver, and germ cell nuclear extracts of old mice (Intano et al., 2003). Also, another large study, using human peripheral blood lymphocytes from over 100 individuals aged 20 to 60 years, showed an age-dependent decline of UV light damage repair (Wei et al., 1993; Grossman and Wei, 1995). The rate of decline was 0.63% per year, which amounts to a 25% decrease over a 40-year period (Wei et al., 1993; Grossman and Wei, 1995).

Higher Rates of Microsatellite Instability in Plants Are Not Due to Lower Efficiency of Replicative DNA Polymerases

DNA replication is a precise process, with DNA replicative polymerases incorporating incorrect bases at a rate of 10^{-6} to 10^{-7} per bp replicated. MMR fixes most of these errors, reducing the error rate additionally by approximately 1,000-fold. In repetitive tracts

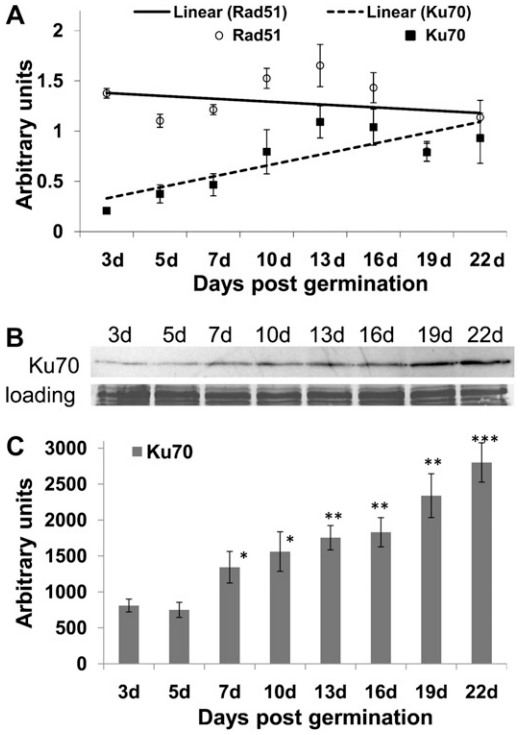

Figure 6. Older plants have higher levels of *Ku70* expression and lower levels of *Rad51* expression. A, cDNA prepared from 3-, 5-, 7-, 10-, 13-, 16-, 19-, and 22-d-old plants was used for the amplification of *Ku70* and *Rad51*. Amplification of tubulin was used as a control. Three independent PCRs using cDNA prepared from three biological repeats were performed. The graph shows the average intensity (in arbitrary units ± SD) of amplified fragments as related to the intensity of tubulin calculated from three independent experiments. Lines show trend lines for *Ku70* (dashed line) and *Rad51* (solid line). B, Western-blot analysis of the amount of KU70 was performed from protein extracts prepared from plants of different ages. The image shows a representative blot. Silver staining of the gel shows equal loading. C, Average expression (in arbitrary units with SD) as quantified from three independent western blots and prorated to the loading controls. Asterisks show significant differences in 5- to 22-d-old plants as compared with 3-d-old plants (* $P < 0.05$, ** $P < 0.01$, *** $P < 0.001$).

that are prone to slippage and mispairing during replication (Kunkel and Bebenek, 2000), potential frameshift mutations including deletions or insertions are more frequent.

Our experiments showed that 21-d-old plants had lower DNA polymerase activity but higher DNA polymerase fidelity. These data were paralleled with a decrease in the expression of all tested replicative polymerases. An age-dependent decrease observed in the expression pattern of replicative DNA polymerases in plants is a novel finding. Similar results have been reported in animals; several reports showed reduced abundance of the replicative DNA polymerase β in brain extracts from older mice and rats (Krishna et al., 2005). For example, the expression of DNA polymerase β and AP endonuclease was induced by DNA damage in young mice, while older mice showed a lack of inducibility (Cabelof et al., 2002).

Unfortunately, no data exist on age-dependent changes in DNA polymerase fidelity in plants. In contrast, several previous reports suggest the existence of lower DNA polymerase activity in older plants (Bottomley, 1970) and aging seeds (Grilli et al., 1995; Reuzeau et al., 1997), thus confirming our findings.

Our finding of the higher fidelity of DNA polymerases in extracts from old plants is puzzling. Since we observed that both RNA levels of major DNA replicative polymerases and the total activity of DNA polymerases dropped with age, it would be logical to expect a drop in the fidelity. It seems that an increase in fidelity could be some kind of compensatory mechanism for lower abundance and activity. We can only hypothesize that higher mutation rates in microsatellites in older plants are not due to the decreased fidelity of replicative DNA polymerases.

The argument for the role of the replication process in the accumulation of heritable mutations is a long-lasting one. The notion that replication errors are the main contributors to heritable mutations in animals seems compelling (Crow, 2000). In contrast, analysis of evolutionary rates of neutral DNA sequences among various plant taxa suggests that more heritable base substitution mutations occur per unit of time during seed ageing than during the lifetime of the plant. This suggests that the higher percentage of heritable mutations is the result of accumulated DNA damage in seeds rather than the result of replication errors occurring upon multiple cell divisions in meristematic regions of growing plants (Whittle, 2006).

Changes in Mismatch Repair May Be Responsible for an Age-Dependent Increase in Microsatellite Instability

Mismatch repair is one of the first DNA repair mechanisms taking care of replicative errors. We thus hypothesized that mistakes in mismatch repair could be more frequent in older plants than in younger plants. As anticipated, our analysis showed that microsatellite mutations occur more frequently in *msh2* plants than in wild-type plants. Alou et al. (2004) also reported that knockout of *AtPMS1* showed up to a 28-fold increase in microsatellite instability. The analysis of the number of blue spots showed that an age-dependent increase in mutation rates was similar in *msh2* and wild-type plants. We should admit, however, that since the number of events in *msh2* plants was so high, it was difficult to make a comprehensive analysis.

The analysis of steady-state RNA levels showed a drastic age-dependent decrease in the expression of *MSH2* and *MSH6* genes and a tendency for increased expression of the *MSH7* gene. Despite phylogenetic evidence that MSH7 arose from MSH6, the mismatch recognition properties of AtMSH2·MSH6 and AtMSH2·MSH7 appeared to differ sharply. The AtMSH2·MSH7 dimer bound poorly to DNA containing a single extra "looped out" nucleotide, whereas this substrate was effectively recognized by AtMSH2·MSH6 (Wu et al., 2003). In contrast, both pairs recognized the G/T mismatch equally well. A decrease in the expression of *MSH2* and *MSH6* but not *MSH7* could possibly suggest that small loops are less efficiently repaired in older plants as compared with younger ones, whereas the repair of mismatches might have similar efficiency. The replication of microsatellites such as G16 frequently results in polymerase slippage leading to single nucleotide deletions or insertions, thus resulting in the formation of single nucleotide loops. Since AtMSH2·MSH6 is responsible for the repair of such loops, it is possible that an age-dependent decrease in the expression of *MSH2* and *MSH6* could contribute to an age-dependent increase in microsatellite instability. However, since there is no in vitro DNA repair assay for the analysis of mismatch repair, it is hard to draw a clear conclusion.

An Age-Dependent Increase in Microsatellite Instability Could Be Due to More Frequent Involvement of NHEJ

Our repair assay showed that older plants have more efficient NHEJ repair as compared with younger plants. At the same time, older plants appeared to be sloppier in end-joining repair as compared with younger plants. These changes were paralleled by the higher steady-state level of *Ku70* RNA and the amount of KU70 protein. These results suggest that older plants indeed use NHEJ repair more often. Since NHEJ is a more error-prone mechanism of end-joining repair as compared with HR repair (Gorbunova and Levy, 1997; Bleuyard et al., 2006), it can be hypothesized that an increase in the involvement of NHEJ repair could be one of the reasons explaining why microsatellite mutations occur in older plants more often.

Our previous work also suggested that older plants utilize NHEJ more frequently. Previously, we found that homologous recombination rates in plants harvested at 2 dpg decreased by 6-fold compared with

plants harvested at 22 dpg (Boyko et al., 2006b). We noticed that whereas the expression of genes involved in recombination repair decreased with age, the expression of genes involved in NHEJ repair increased (Boyko et al., 2006b).

Microsatellites are often subject to frequent unequal crossing over. Unequal crossing over between direct repeats involves misaligned pairing of repeats on homologous chromosomes (Lovett, 2004). It can be hypothesized that a decrease in the involvement of HR could be one of the protection mechanisms preventing frequent rearrangements/crossing over that could contribute to microsatellite instability.

Unfortunately, not much is known about age-dependent changes in strand break repair in plants. In animals, the efficiency of NHEJ was reduced over 4-fold in presenescent and senescent cells relative to young cells, indicating that DNA end joining becomes less efficient and more error prone in senescent cells (Seluanov et al., 2004). The level of *Ku70* has been shown to decline markedly in the testes of aging rats (Um et al., 2003) and lymphocytes from aging human donors (Ju et al., 2006). Also, in a recent publication, a 50% reduction in the level of KU70 and KU80 proteins in senescent human fibroblasts was observed (Seluanov et al., 2007). Analysis of NHEJ in the brains of young and old rats using the in vitro plasmid rejoining assay showed a substantial reduction in the efficiency of plasmid rejoining in the brains of old rats (Ren and Peña de Ortiz, 2002; Vyjayanti and Rao, 2006). A similar experiment described in this paper also showed that end-joining repair was more error prone in older plants. At the same time, we found that older plants use NHEJ more often than younger plants.

CONCLUSION

Our experiments showed that microsatellite instability in plants increased with age. Further analysis showed that there was a correlation between the more frequent involvement of NHEJ and higher microsatellite instability in older plants. Since we observed a decrease in the expression of genes coding for MMR, it cannot be excluded that a lower capacity of MMR contributes to higher mutation rates in older plants. It remains to be shown whether mutants impaired in NHEJ would be impaired in an age-dependent increase in microsatellite mutation rates.

MATERIALS AND METHODS

Plant Lines and Growing Conditions

Production of the Arabidopsis (*Arabidopsis thaliana*) microsatellite instability reporter line 121A has been described previously (Azaiez et al., 2006). Briefly, this line contains a synthetic microsatellite (16 Gs) cloned into the *uidA* gene's *Msc*I restriction site, 620 bp downstream of the start codon. This generates a premature stop codon at the position of eight nucleotides downstream of the cloned fragment. The loss of a single nucleotide or the gain of two nucleotides at the microsatellite locus will provide the correct frameshift to activate the GUS gene (Fig. 1). Seeds from line 121A were sown on Murashige and Skoog medium (Sigma) plates and grown under controlled light and temperature conditions (16 h of light at 22°C and 8 h of dark at 18°C with illumination of 200 μmol m^{-2} s^{-1}). Plants were harvested on days 3, 5, 7, 10, 13, 16, 19, and 22 post germination.

For the analysis of the role of MMR, line121A was crossed to the *msh2* mutant (Azaiez et al., 2006), homozygous lines were selected, and the frequency of mutations in the microsatellite region was measured at the aforementioned days post germination.

Histochemical Staining Procedures

Histochemical staining of plants was performed at the aforementioned developmental stages as described before (Jefferson et al., 1987). Briefly, the plants were vacuum infiltrated for 10 min in a sterile staining buffer containing 100 mg of 5-bromo-4-chloro-3-indolyl glucuronide substrate (Jersey Labs) in 300 mL of 100 mM phosphate buffer (pH 7.0), 0.05% NaN_3, 0.05% Tween 80, and 1 mL of dimethylformamide. The plants were then incubated at 37°C for 48 h in the staining buffer and bleached with ethanol (Fig. 1B).

Calculating the Number of Genomes

Total DNA from various transgenic lines was isolated from whole plants at different developmental stages using the Nucleon Phytopure plant DNA extraction kit (Amersham Life Science). To estimate the number of genomes present, the total DNA yield (μg $plant^{-1}$) was compared with the DNA content of an Arabidopsis cell (0.16 pg; Swoboda et al., 1993).

To find out whether the DNA extraction method had a significant influence on yield, we prepared DNA using an additional previously published protocol (Boyko et al., 2006a, 2006b). Although the DNA yield was increased by 50% as compared with the yield produced by the Nucleon Phytopure kit, the ratio between the amounts of DNA in different plant organs was the same.

Preparation of Plant Crude Tissue Extracts for the Analysis of DNA Polymerase Activity

Leaves from 5-, 12-, and 21-d-old plants of line 121A were used for the preparation of crude extracts. All extraction steps were carried out on ice. Using a pestle and mortar, 10 g of leaves was homogenized with 100 mL of prechilled homogenization buffer (100 mM sodium phosphate buffer, pH 7.4, containing 1% [v/v] protease inhibitor cocktail from Sigma [P9599-5ML]) to obtain a 10% extract. The extracts were filtered through four layers of cheesecloth and centrifuged at 10,000 rpm for 15 min. The supernatant obtained was immediately used for assays. If necessary, crude plant extracts can be partially purified using any suitable method (for instance, the one described by Li et al. [2002]). For the analysis of total protein concentration in crude plant tissue extracts, the Bradford assay with bovine serum albumin as a standard was applied (Bradford, 1976). The experiments were repeated three times.

Preparation of the Primer/Template Complex

The primer/template complex for the assay was prepared by annealing the fluorescein amidite (FAM)-labeled 15-bp primer (5′-6-FAM-TCCCAGTCACGACGT-3′; PAGE purified) to the 30-bp template (5′-TCATCGAGCATGATCACGTCGTGACTGGGA-3′; PAGE purified). All components were mixed by pipetting in the following order (on ice): ΣV = 200 μL, Tris-HCl (1 M, pH 8.0) = 10 μL, β-mercaptoethanol (14.3 M) = 0.5 μL, BSA (10 mg mL^{-1}; New England Biolabs) = 2 μL, primer (100 μM) = 3 μL, template (100 μM) = 3 μL, water = 183.5 μL. The reaction was incubated for 5 min in boiling water and then allowed to cool to room temperature (20°C–25°C). The complex was prepared in advance and stored at −20°C.

Polymerization Reaction

The crude extract (10 μg of total protein) was mixed with the primer/template complex, 2 mM deoxyribonucleotide triphosphate (dNTP), and reaction buffer (10× Y+/Tango; Fermentas), 10 mM magnesium acetate, 66 mM potassium acetate, 0.1 mg mL^{-1} BSA: ΣV = 25 μL, dNTP (2 mM) = 2.5 μL, template/primer complex = 2.5 μL, reaction buffer = 2.5 μL, plant extract = 10 μg of total protein, water = 25 μL.

The reaction was carried out at 37°C for 15 min in a PCR machine, quenched with 50 μL of loading buffer (95% formamide, 50 mM EDTA, and 0.05% bromphenol blue), heated to 95°C for 3 min, and cooled on ice for 2 min. The Klenow enzyme (New England Biolabs buffer 2) was used as a positive control.

Denaturing PAGE and Gel Scanning

After quenching, 15 μL of the sample/loading buffer mix was loaded on a 20% polyacrylamide gel (20 × 20 × 0.075 cm) containing 8 M urea. Also, 0.5 μL of the 15-bp 6-FAM-labeled primer was mixed with 2.5 μL of loading buffer and loaded on the polyacrylamide gel to serve as a M_r marker. Electrophoresis was carried out in 1× Tris-borate/EDTA buffer for about 5 h at 500 V. Gels were scanned using Typhoon 9410 at an excitation wavelength of 88 nm using a 520 BP 40 emission filter, photomultiplier voltage of 685 V, at a resolution of 100 μm. Images of scanned gels were analyzed using ImageQuant 5.2 software (Molecular Dynamics). For the adjustment of total values of the object outline, the local median background correction method was applied.

Real-Time PCR Analysis

Approximately 80 mg of plant tissue was ground in liquid nitrogen and transferred to a chilled 1.5-mL Eppendorf tube, and 160 μL of TRIzol reagent (Invitrogen) was added. The remainder of the extraction was performed as per the manufacturer's protocol. RNA quantity and quality were measured using a spectrophotometer (Ultraspec 1100 pro) in 20 mM Tris, pH 7.5, in RNase-free double distilled water. cDNA was then prepared from total RNA using the RevertAID H First Strand cDNA synthesis kit (Fermentas).

Real-time quantitative PCR was performed using SsoFast EvanGreen Supermix (Bio-Rad). cDNAs were amplified under the following conditions: (1) 98°C for 3 min for one cycle; (2) 98°C for 5 s, 54.3°C for 5 s, 65°C to 95°C for 5 s, with a 0.5°C increment for 40 cycles. Primers (Supplemental Table S3) for real-time quantitative PCR were designed using the Primer3 program. For every set of primers, annealing temperature optimization, melt curve analysis, and gel analysis of amplicons were performed. To evaluate PCR efficiency, the standard curve was established using a series of cDNA dilutions. The expression of polymerases was related to the expression of *RCE1*. Conditions of *RCE1* amplification were as follows: (1) 98°C for 3 min for one cycle; (2) 98°C for 5 s, 45.0°C for 5 s, 65°C to 95°C for 5 s, with a 0.5°C increment for 46 cycles. The expression of *RCE1* is commonly used for the analysis of expression of developmentally or metabolically regulated genes (Seki et al., 2001). The average of four reactions (two dilutions per each of two RNA preparations) was obtained, and the fold induction was calculated. The statistical significance of the experiment was confirmed by performing Student's *t* test (two-tailed paired or nonpaired).

Partial Plant Extract Purification for the in Vitro DNA Repair Assay

All steps were performed on ice. Frozen plant tissues from 5-, 12-, and 21-d-old plants were ground with liquid nitrogen and resuspended in 7 volumes (w/v) of ice-cold homogenization buffer (25 mM HEPES-KOH, pH 7.8, 100 mM KCl, 5 mM $MgCl_2$, 250 mM Suc, 10% glycerol, 1 mM dithiothreitol, and the protease inhibitor cocktail Complete Mini [Roche]). The homogenates were filtered through 45-μm filters and placed on a magnetic stirrer. KCl (2 M) was added slowly to the stirring homogenates to a final concentration of 450 mM. After 30 min of extraction, the homogenates were centrifuged at 40,000*g* for 1 h to remove cellular and nuclear debris. The supernatants were transferred to glass beakers, and solid $(NH_4)_2SO_4$ was added slowly to a final concentration of 70%. Ten microliters of 1 M NaOH was added for each 1 g of $(NH_4)_2SO_4$ to neutralize the supernatant. After 1 h of incubation on ice, the precipitated proteins were collected by centrifugation at 20,000*g* for 1 h. The supernatants were discarded, and the pellets were dissolved in a minimum volume (3 mL) of a dialysis buffer (25 mM HEPES-KOH, pH 7.8, 100 mM KCl, 12 mM $MgCl_2$, 1 mM EDTA, 17% glycerol, and 2 mM dithiothreitol) and dialyzed overnight against the same buffer (in 4 L) using 7,000 MWCO Slide-A-Lyser dialysis cassettes (Thermo Scientific). After dialysis, the samples were split into aliquots, frozen in liquid nitrogen, and kept at −80°C.

In Vitro Repair Assay

All reactions were done in triplicate. LITMUS29 (New England Biolabs) was used in the experiments. Circular, linearized, blunt-ended (*Stu*I; Fermentas) nondamaged and damaged plasmids (UV light, λ_{max} = 254 nm, 450 J m^{-2}) as well as linearized, non-sticky-ended (*Bam*HI/*Kpn*I; Fermentas) nondamaged and damaged plasmids (UV light, λ_{max} = 254 nm, 450 J m^{-2}) were used for the assay. Each reaction (25 μL total volume) contained one form of plasmid DNA (300 ng $reaction^{-1}$), 2.5 μL of 10× reaction buffer (Roche), 2.5 μL of 10× dNTP/DIG-11-dUTP mix (Roche), and 10 μg of a partially purified plant extract (Li et al., 2002). Plant extracts were prepared from 5-, 12-, and 21-d-old plants (10 plants per each sample). Reaction mixes were incubated in the dark for 2 h at 25°C. The reactions were stopped with 20 mM EDTA (the final concentration). DNA (120 ng) was separated by electrophoresis in 0.8% agarose/1× Tris-acetate EDTA, visualized with ethidium bromide, photographed, and transferred to a nylon membrane (Roche) in 10× SSC solution using a vacuum blotter (Appligene; Supplemental Fig. S3). After transfer, DNA was bound to a membrane by UV light using a Spectrolinker XL-1000 (Spectronics) and detected with the DIG Nucleic Acid Detection kit (Roche) using anti-digoxigenin-alkaline phosphatase conjugate and nitroblue tetrazolium/5-bromo-4-chloro-3-indolyl phosphate as a substrate according to the manufacturer's instructions (Roche). Membranes were scanned and quantified with ImageJ.

Analysis of Strand Break Repair Using Plant Protoplasts

Protoplasts were prepared from leaves of 5-, 12-, and 21-d-old Arabidopsis plants and transfected essentially as described (Pelczar et al., 2003). For the analysis, the pGEM (Promega) plasmid carrying the ampicillin resistance gene and the *LacZ* gene was digested with *Kpn*I to generate 3′ protruding ends. Digested DNA was purified from the gel and dephosphorylated; the absence of a circular plasmid molecule was tested by PCR across the restriction site region (data not shown). Protoplasts of 5-, 12-, and 21-d-old plants were transfected with 5 μg of linear DNA. To normalize for equal transfection efficiency, each protoplast sample was also transfected with 0.5 μg of circular pM1-Luc (Roche) plasmid carrying a kanamycin resistance gene.

Materials were added to 15-mL Falcon tubes in the following order: 5.5 μg of DNA, 0.3 mL of a suspension containing 1.0×10^6 protoplasts mL^{-1}, and 0.3 mL of 40% polyethylene glycol 6000. The mix was incubated for 5 min at room temperature, and then 4 mL of K3 medium was added. After mixing, the tubes were incubated in a horizontal position at 28°C in the dark. Incubation was performed for 4 and 12 h. Harvesting of transfected protoplasts was done using 10 mL of W5 buffer (150 mM NaCl, 125 mM $CaCl_2$, 5 mM KCl, and 6 mM Glc) and by centrifugation for 10 min at 1,000 rpm. The Qiagen Miniprep kit was used to purify the circular form of DNA. This DNA was used for *Escherichia coli* transformation.

Following transformation, 90% of the bacteria were plated on ampicillin-containing medium and the remainder were plated on kanamycin-containing medium supplemented with X-Gal/isopropylthio-β-galactoside. The number of ampicillin-resistant and kanamycin-resistant bacterial colonies was counted and compared between different age groups. The number of kanamycin-resistant bacterial colonies was equal in all samples prepared from protoplasts of different ages, suggesting that protoplast transfection steps, DNA recovery steps, and bacteria transfection steps were similarly efficient in all three protoplast groups.

Western Immunoblotting

Western-blot analysis of the amount of KU70 was performed from approximately 100 mg of plant tissue using anti-KU70 primary antibodies (1:500; Santa Cruz Biotechnology) and anti-goat secondary antibodies (1:5,000; Santa Cruz Biotechnology) as described before (Boyko et al., 2006b).

Statistical Analysis

The experiments were repeated at least three times, and mean values ± SD or SE were calculated. The statistical significance of the results was confirmed by performing Student's *t* test. Statistical analyses were performed using Microcal Origin 6.0.

Supplemental Data

The following materials are available in the online version of this article.

Supplemental Figure S1. Representative chromatograms.

Supplemental Figure S2. A general outline of the experiment.

Supplemental Figure S3. Loading controls.

Supplemental Table S1. Microsatellite mutation frequency, the number of genomes, and microsatellite rates in plants of different ages.

Supplemental Table S2. Comparison of the increase in mutation rate with age in wild-type and *msh2* Arabidopsis plants.

Supplemental Table S3. Primers and melting temperatures.

ACKNOWLEDGMENTS

We thank Valentina Titova for proofreading the manuscript.

Received July 16, 2010; accepted August 24, 2010; published September 3, 2010.

LITERATURE CITED

Alou AH, Azaiez A, Jean M, Belzile FJ (2004) Involvement of the Arabidopsis thaliana AtPMS1 gene in somatic repeat instability. Plant Mol Biol **56:** 339–349

Arabidopsis Genome Initiative (2000) Analysis of the genome sequence of the flowering plant Arabidopsis thaliana. Nature **408:** 796–815

Azaiez A, Bouchard EF, Jean M, Belzile FJ (2006) Length, orientation, and plant host influence the mutation frequency in microsatellites. Genome **49:** 1366–1373

Ben Yehuda A, Globerson A, Krichevsky S, Bar On H, Kidron M, Friedlander Y, Friedman G, Ben Yehuda D (2000) Ageing and the mismatch repair system. Mech Ageing Dev **121:** 173–179

Blanc G, Barakat A, Guyot R, Cooke R, Delseny M (2000) Extensive duplication and reshuffling in the *Arabidopsis* genome. Plant Cell **12:** 1093–1101

Bleuyard JY, Gallego ME, White CI (2006) Recent advances in understanding of the DNA double-strand break repair machinery of plants. DNA Repair (Amst) **5:** 1–12

Boldyrev A, Bulygina E, Gerassimova O, Lyapina L, Schoner W (2004) Functional relationship between Na/K-ATPase and NMDA-receptors in rat cerebellum granule cells. Biochemistry (Mosc) **69:** 429–434

Bottomley W (1970) Deoxyribonucleic acid-dependent ribonucleic acid polymerase activity of nuclei and plastids from etiolated peas and their response to red and far red light in vivo. Plant Physiol **45:** 608–611

Boyko A, Filkowski J, Hudson D, Kovalchuk I (2006a) Homologous recombination in plants is organ specific. Mutat Res **595:** 145–155

Boyko A, Zemp F, Filkowski J, Kovalchuk I (2006b) Double-strand break repair in plants is developmentally regulated. Plant Physiol **141:** 488–497

Bradford MM (1976) A rapid and sensitive method for the quantitation of microgram quantities of protein utilizing the principle of protein-dye binding. Anal Biochem **72:** 248–254

Britt AB (1996) DNA damage and repair in plants. Annu Rev Plant Physiol Plant Mol Biol **47:** 75–100

Cabelof DC, Raffoul JJ, Yanamadala S, Ganir C, Guo Z, Heydari AR (2002) Attenuation of DNA polymerase beta-dependent base excision repair and increased DMS-induced mutagenicity in aged mice. Mutat Res **500:** 135–145

Chwedorzewska KJ, Bednarek PT, Puchalski J (2002a) Studies on changes in specific rye genome regions due to seed aging and regeneration. Cell Mol Biol Lett **7:** 569–576

Chwedorzewska KJ, Bednarek PT, Puchalski J, Krajewski P (2002b) AFLP-profiling of long-term stored and regenerated rye GenBank samples. Cell Mol Biol Lett **7:** 457–463

Crow JF (2000) The origins, patterns and implications of human spontaneous mutation. Nat Rev Genet **1:** 40–47

Gorbunova V, Levy AA (1997) Non-homologous DNA end joining in plant cells is associated with deletions and filler DNA insertions. Nucleic Acids Res **25:** 4650–4657

Gorbunova V, Seluanov A, Mao Z, Hine C (2007) Changes in DNA repair during aging. Nucleic Acids Res **35:** 7466–7474

Grilli M, Ribola M, Alberici A, Valerio A, Memo M, Spano P (1995) Identification and characterization of a kappa B/Rel binding site in the regulatory region of the amyloid precursor protein gene. J Biol Chem **270:** 26774–26777

Grossman L, Wei Q (1995) DNA repair and epidemiology of basal cell carcinoma. Clin Chem **41:** 1854–1863

Hays JB (2002) Arabidopsis thaliana, a versatile model system for study of eukaryotic genome-maintenance functions. DNA Repair (Amst) **1:** 579–600

Intano GW, Cho EJ, McMahan CA, Walter CA (2003) Age-related base excision repair activity in mouse brain and liver nuclear extracts. J Gerontol A Biol Sci Med Sci **58:** 205–211

Jefferson RA, Kavanagh TA, Bevan MW (1987) GUS fusions: beta-glucuronidase as a sensitive and versatile gene fusion marker in higher plants. EMBO J **6:** 3901–3907

Ju YJ, Lee KH, Park JE, Yi YS, Yun MY, Ham YH, Kim TJ, Choi HM, Han GJ, Lee JH, et al (2006) Decreased expression of DNA repair proteins Ku70 and Mre11 is associated with aging and may contribute to the cellular senescence. Exp Mol Med **38:** 686–693

Karran P (1996) Microsatellite instability and DNA mismatch repair in human cancer. Semin Cancer Biol **7:** 15–24

Kovalchuk I, Pelczar P, Kovalchuk O (2004) High frequency of nucleotide misincorporations upon the processing of double-strand breaks. DNA Repair (Amst) **3:** 217–223

Krichevsky S, Pawelec G, Gural A, Effros RB, Globerson A, Yehuda DB, Yehuda AB (2004) Age related microsatellite instability in T cells from healthy individuals. Exp Gerontol **39:** 507–515

Krishna TH, Mahipal S, Sudhakar A, Sugimoto H, Kalluri R, Rao KS (2005) Reduced DNA gap repair in aging rat neuronal extracts and its restoration by DNA polymerase beta and DNA-ligase. J Neurochem **92:** 818–823

Kunkel TA, Bebenek K (2000) DNA replication fidelity. Annu Rev Biochem **69:** 497–529

Li A, Schuermann D, Gallego F, Kovalchuk I, Tinland B (2002) Repair of damaged DNA by *Arabidopsis* cell extract. Plant Cell **14:** 263–273

Lovett ST (2004) Encoded errors: mutations and rearrangements mediated by misalignment at repetitive DNA sequences. Mol Microbiol **52:** 1243–1253

Marriage TN, Hudman S, Mort ME, Orive ME, Shaw RG, Kelly JK (2009) Direct estimation of the mutation rate at dinucleotide microsatellite loci in Arabidopsis thaliana (Brassicaceae). Heredity **103:** 310–317

Meinke DW, Cherry JM, Dean C, Rounsley SD, Koornneef M (1998) Arabidopsis thaliana: a model plant for genome analysis. Science **282:** 662–682

Melletti G, Russo C (1969) A rare case of extramedullary gastric plasmocytoma. Rass Int Clin Ter **49:** 1442–1450

Mitchell DL, Hartman PS (1990) The regulation of DNA repair during development. Bioessays **12:** 74–79

Neri S, Gardini A, Facchini A, Olivieri F, Franceschi C, Ravaglia G, Mariani E (2005) Mismatch repair system and aging: microsatellite instability in peripheral blood cells from differently aged participants. J Gerontol A Biol Sci Med Sci **60:** 285–292

Pelczar P, Kalck V, Kovalchuk I (2003) Different genome maintenance strategies in human and tobacco cells. J Mol Biol **331:** 771–779

Peto FH (1933) The effect of aging and heat on the chromosomal mutation rates in maize and barley. Can J Res **9:** 261–264

Ren K, Peña de Ortiz S (2002) Non-homologous DNA end joining in the mature rat brain. J Neurochem **80:** 949–959

Reuzeau C, McNally JG, Pickard BG (1997) The endomembrane sheath: a key structure for understanding the plant cell? Protoplasma **200:** 1–9

Seki M, Narusaka M, Abe H, Kasuga M, Yamaguchi-Shinozaki K, Carninci P, Hayashizaki Y, Shinozaki K (2001) Monitoring the expression pattern of 1300 *Arabidopsis* genes under drought and cold stresses by using a full-length cDNA microarray. Plant Cell **13:** 61–72

Seluanov A, Danek J, Hause N, Gorbunova V (2007) Changes in the level and distribution of Ku proteins during cellular senescence. DNA Repair (Amst) **6:** 1740–1748

Seluanov A, Mittelman D, Pereira-Smith OM, Wilson JH, Gorbunova V (2004) DNA end joining becomes less efficient and more error-prone during cellular senescence. Proc Natl Acad Sci USA **101:** 7624–7629

Shinde D, Lai Y, Sun F, Arnheim N (2003) Taq DNA polymerase slippage mutation rates measured by PCR and quasi-likelihood analysis: (CA/GT)n and (A/T)n microsatellites. Nucleic Acids Res **31:** 974–980

Sia EA, Jinks-Robertson S, Petes TD (1997) Genetic control of microsatellite stability. Mutat Res **383:** 61–70

Swoboda P, Hohn B, Gal S (1993) Somatic homologous recombination in planta: the recombination frequency is dependent on the allelic state of recombining sequences and may be influenced by genomic position effects. Mol Gen Genet **237:** 33–40

Thuillet AC, Bru D, David J, Roumet P, Santoni S, Sourdille P, Bataillon T (2002) Direct estimation of mutation rate for 10 microsatellite loci in durum wheat, Triticum turgidum (L.) Thell. ssp durum desf. Mol Biol Evol **19:** 122–125

Tuteja N, Singh MB, Misra MK, Bhalla PL, Tuteja R (2001) Molecular mechanisms of DNA damage and repair: progress in plants. Crit Rev Biochem Mol Biol **36:** 337–397

Um JH, Kim SJ, Kim DW, Ha MY, Jang JH, Kim DW, Chung BS, Kang CD, Kim SH (2003) Tissue-specific changes of DNA repair protein Ku and mtHSP70 in aging rats and their retardation by caloric restriction. Mech Ageing Dev **124:** 967–975

Viguera E, Canceill D, Ehrlich SD (2001) Replication slippage involves DNA polymerase pausing and dissociation. EMBO J **20:** 2587–2595

Vyjayanti VN, Rao KS (2006) DNA double strand break repair in brain: reduced NHEJ activity in aging rat neurons. Neurosci Lett **393:** 18–22

Wei Q, Matanoski GM, Farmer ER, Hedayati MA, Grossman L (1993) DNA repair and aging in basal cell carcinoma: a molecular epidemiology study. Proc Natl Acad Sci USA **90:** 1614–1618

Whittle CA (2006) The influence of environmental factors, the pollen:ovule ratio and seed bank persistence on molecular evolutionary rates in plants. J Evol Biol **19:** 302–308

Whittle CA, Beardmore T, Johnston MO (2001) Is G1 arrest in plant seeds induced by a p53-related pathway? Trends Plant Sci **6:** 248–251

Whittle CA, Johnston MO (2006) Moving forward in determining the causes of mutations: the features of plants that make them suitable for assessing the impact of environmental factors and cell age. J Exp Bot **57:** 1847–1855

Wu SY, Culligan K, Lamers M, Hays J (2003) Dissimilar mispair-recognition spectra of Arabidopsis DNA-mismatch-repair proteins MSH2*MSH6 (MutSalpha) and MSH2*MSH7 (MutSgamma). Nucleic Acids Res **31:** 6027–6034